



HAL
open science

Influence of Donor-Substituents on Triphenylamine Chromophores Bearing Pyridine Fragments

Jiri Tydlitat, Michaela Fecková, Pascal Le Poul, Oldrich Pytela, Milan Klikar, Julian Rodriguez-Lopez, Françoise Robin-Le Guen, Sylvain Achelle

► **To cite this version:**

Jiri Tydlitat, Michaela Fecková, Pascal Le Poul, Oldrich Pytela, Milan Klikar, et al.. Influence of Donor-Substituents on Triphenylamine Chromophores Bearing Pyridine Fragments. *European Journal of Organic Chemistry*, 2019, 2019 (9), pp.1921-1930. 10.1002/ejoc.201900026 . hal-02086459

HAL Id: hal-02086459

<https://univ-rennes.hal.science/hal-02086459v1>

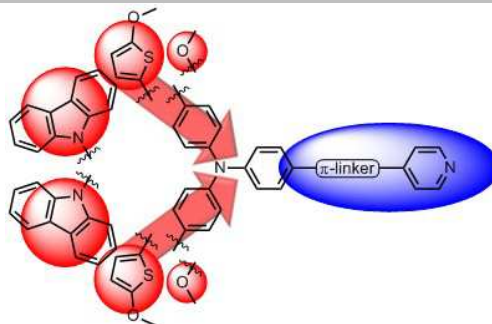
Submitted on 16 Apr 2019

HAL is a multi-disciplinary open access archive for the deposit and dissemination of scientific research documents, whether they are published or not. The documents may come from teaching and research institutions in France or abroad, or from public or private research centers.

L'archive ouverte pluridisciplinaire **HAL**, est destinée au dépôt et à la diffusion de documents scientifiques de niveau recherche, publiés ou non, émanant des établissements d'enseignement et de recherche français ou étrangers, des laboratoires publics ou privés.

FULL PAPER

A series of push-pull chromophores with a pyridine electron-withdrawing fragment and methoxy-, 9*H*-carbazol-9-yl- and 5-methoxythiophen-2-yl-substituted diphenylamino groups as electron-donating units was designed.



Push-pull chromophores

Jiří Tydlitát,^{*} Michaela Fecková,
Pascal le Poul, Oldřich Pytela,
Milan Klikar, Julián Rodríguez-
López,^{*} Françoise Robin-le Guen
and Sylvain Achelle[†]

Page No. – Page No.

**Influence of donor-substituents
on triphenylamine
chromophores bearing pyridine
fragments**

Influence of donor-substituents on triphenylamine chromophores bearing pyridine fragments

Jiří Tydlitát,^{*,a} Michaela Fecková,^{a,b} Pascal le Poul,^b Oldřich Pytela,^a Milan Klikar,^a Julián Rodríguez-López,^{*,c} Françoise Robin-le Guen^b and Sylvain Achelle^{*,b}

^a Dr. Jiří Tydlitát, Michaela Fecková, Prof. Oldřich Pytela, Dr Milan Klikar Institute of Organic Chemistry and Technology, Faculty of Chemical Technology, University of Pardubice, Studentská 573, Pardubice 53210, Czech Republic. jiri.tydlitat@upce.cz
<http://bures.upce.cz/tydlitat.html>

^b Michaela Fecková, Dr. Pascal le Poul, Prof. Françoise Robin-le Guen, Dr. Sylvain Achelle Université de Rennes, CNRS, Institut des Sciences Chimiques de Rennes - UMR6226, F35000 Rennes, France. sylvain.achelle@univ-rennes1.fr <https://iscr.univ-rennes1.fr/omc/dr-sylvain-achelle>

^c Prof. Julián Rodríguez-López Facultad de Ciencias y Tecnologías Químicas, Universidad de Castilla-La Mancha, 13071 Ciudad Real, Spain. julian.rodriguez@uclm.es

Abstract

Efficient synthetic routes that combine different palladium-catalyzed cross-coupling reactions have been developed for the preparation of a new family of push-pull derivatives in which pyridine was used as the acceptor group and different *para*-substituted diphenylamines as the donor groups. All compounds showed absorption in the UV-Vis region and blue-green emission with high quantum yields. Significant red shifts were observed in the absorption and fluorescence emission maxima on increasing the electron-donating ability of the substituents

or on incorporating a π -conjugated linker. This finding can be explained on the basis of enhanced intramolecular charge transfer (ICT). Strong emission solvatochromism confirmed the formation of an intramolecular charge-separated emitting state. The HOMO-LUMO energy gaps have been estimated by experimental electrochemical measurements and the results were interpreted with the aid of DFT calculations. The thermal behavior of all materials has also been studied by differential scanning calorimetry.

Keywords: Luminescence; Nitrogen heterocycles; Charge transfer; Triphenylamine; Solvatochromism

1. Introduction

During the past two decades there has been great interest in the design of push-pull structures based on a π -conjugated core substituted with electron-donating (D) and electron-attracting (A) groups due to their applications in emissive materials for sensors¹ and organic light-emitting diodes (OLEDs),² bulk heterojunction³ and dye-sensitized solar cells (DSSCs),⁴ field effect transistors,⁵ and nonlinear optics (NLO).⁶ The photophysical and electronic properties of push-pull chromophores, which are closely linked to intramolecular charge transfer (ICT) occurring in the molecule, can be easily tuned by tailoring the D/A couple,^{7,8} the π -conjugated linker,^{7,9} or by designing advanced quadrupolar or tripodal arrangements.¹⁰

The diphenylamino group has been extensively used as an electron-donating group in push-pull structures used as emissive materials,^{9b,11} NLO chromophores^{11d,12} and dyes for DSSCs.¹³

The electron-donating strength of the diphenylamino group is lower than that of dialkylamino analogs¹⁴ but the diphenylamino derivatives generally have higher fluorescence quantum yields,^{9b,11d,15} thus making them more interesting for applications related to emission. A significant branching effect that enhances the two-photon absorption (TPA) has been observed on the triphenylamine core,¹⁶ but the polysubstitution of the triphenylamine core by

two of three electron-withdrawing arms generally leads to a blue shift of the emission.^{16b,17} Reinforcing the electron-donating strength of the diphenylamino group would allow red-shifted emission to be obtained while maintaining a high fluorescence quantum yield. The 4-[bis(4-methoxyphenyl)amino]phenyl group has been described by Marder and co-workers as a promising combination of a reasonably high π -donor strength with the high stability previously reported for 4-(diarylamino)phenyl donors.¹⁴ Some examples of methoxy-,¹⁸ diphenylamino-¹⁹ and carbazolyl-^{19a,20} substituted diphenylamino emissive materials have been described in the literature. Nevertheless, to the best of our knowledge, systematic comparisons have not been performed with regards to their unsubstituted analogs.

The pyridine fragment is a moderately strong electron-withdrawing group that can be used in push-pull structures.²¹ The presence of a nitrogen atom with a lone electron pair enables the photophysical properties of pyridine derivatives to be tuned upon protonation, complexation and hydrogen-bond formation. In this context, the incorporation of this heterocycle as an electron-withdrawing fragment in push-pull structures appears to be interesting for the design of fluorescent sensors.²² We recently described acid-responsive triphenylamine derivatives bearing pyridine fragments.²³ White photoluminescence was obtained in solution by controlled protonation of the blue-emitting pyridine derivatives, which resulted in yellow-orange emissive acidified forms.

In the work described here we designed a series of selected methoxy-, 9*H*-carbazol-9-yl- and 5-methoxythiophen-2-yl-substituted triphenylamines **1–6** linked to pyridine fragments and assessed the structure-property relationships. The photophysical and electrochemical properties were compared to those of the recently described²³ unsubstituted triphenylamine analogs **A–C** (Figure 1).

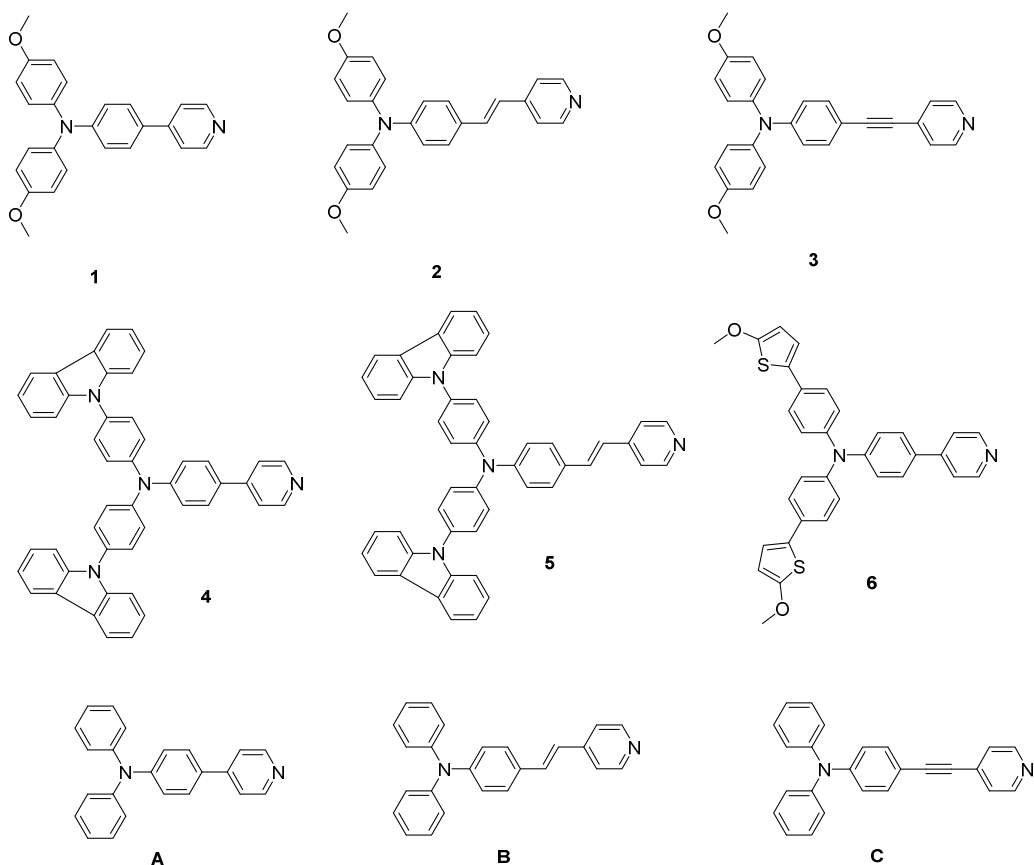
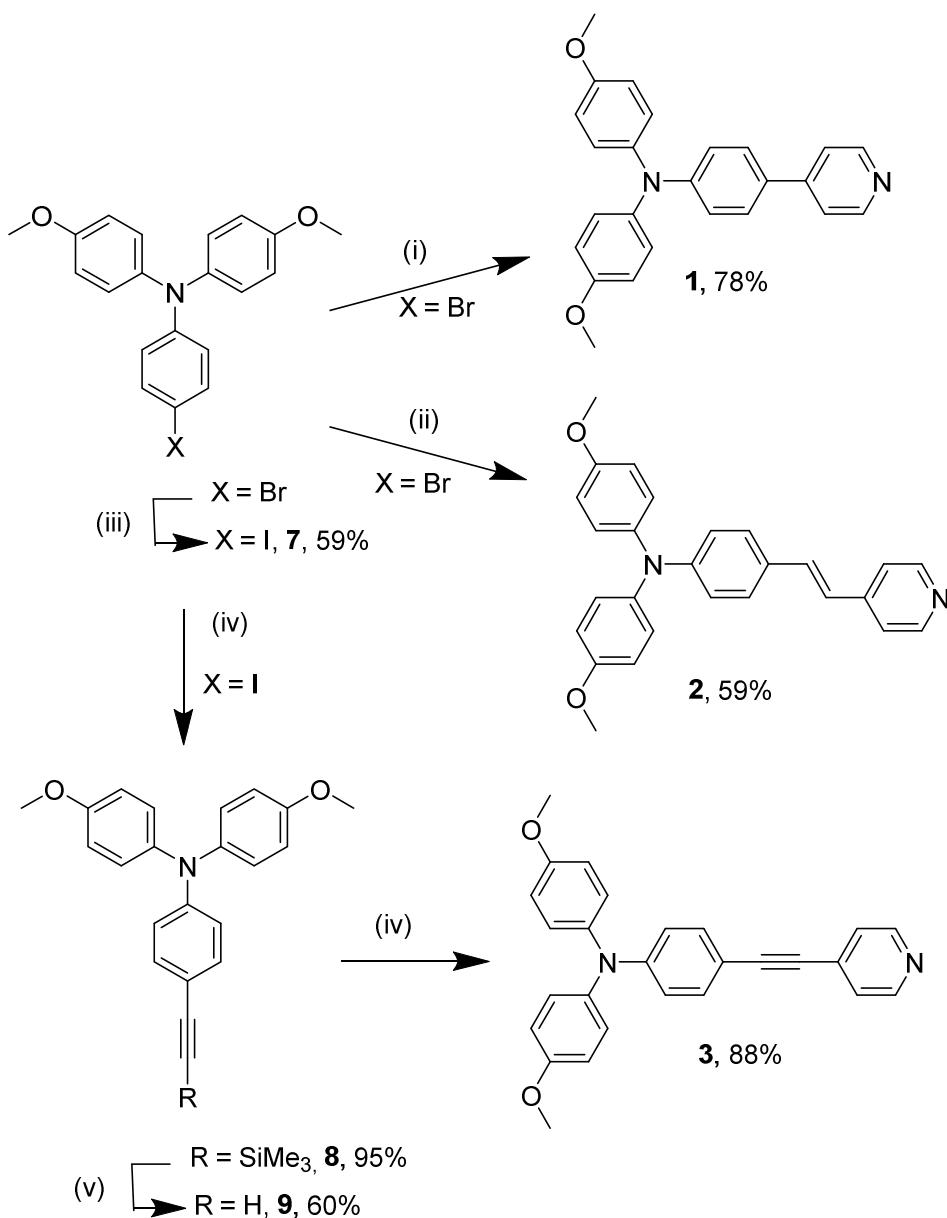


Figure 1. Structures of target compounds **1–6** and their unsubstituted analogs **A–C**.

2. Results and Discussion

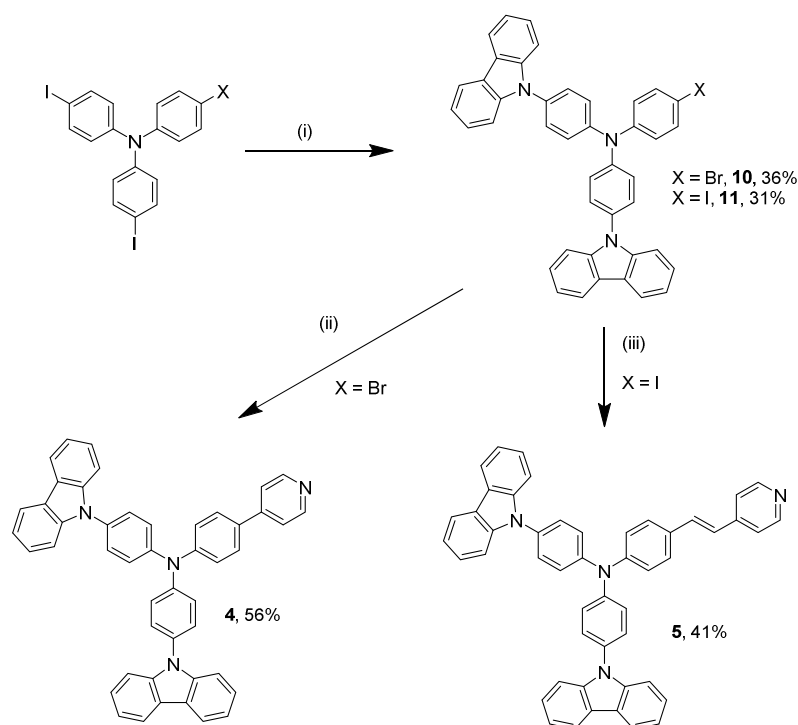
Synthesis. The methoxy-substituted triphenylamine derivatives **1–3** were obtained from commercially available 4-bromo-*N,N*-bis(4-methoxyphenyl)aniline (Scheme 1). The Suzuki–Miyaura cross-coupling reaction with pyridin-4-ylboronic acid gave chromophore **1** in good yield, whereas compound **2** was synthesized in moderate yield by Heck cross-coupling with 4-vinylpyridine according to a reported procedure.²⁴ The synthesis of the acetylenic derivative **3** required a four-step route: a halogen-metal exchange with iodine as electrophile to give iodo-derivative **7**, a Sonogoshira cross-coupling reaction with triphenylsilylacetylene followed by deprotection of the trimethylsilyl group to obtain alkyne **9** and, finally, a second Sonogashira cross-coupling reaction with 4-iodopyridine to afford the target chromophore in good yield.



Scheme 1. (i) pyridin-4-ylboronic acid, $\text{PdCl}_2(\text{PPh}_3)_2$, Na_2CO_3 , dioxane/ H_2O 4:1, Δ , 18 h (ii) 4-vinylpyridine, $\text{Pd}(\text{OAc})_2$, $\text{P}(o\text{-tol})_3$, diethylamine, DMF, 90 °C, 24 h (iii) *n*-Buli, I_2 , THF, –78 °C, 3.5 h (iv) trimethylsilylacetylene, $\text{PdCl}_2(\text{PPh}_3)_2$, CuI, *i*Pr₂NH, 60 °C, 1 h (v) K_2CO_3 , MeOH, rt, 18 h (vi) 4-iodopyridine, $\text{PdCl}_2(\text{PPh}_3)_2$, CuI, dioxane/ Et_3N 4:1, 90 °C, 18 h.

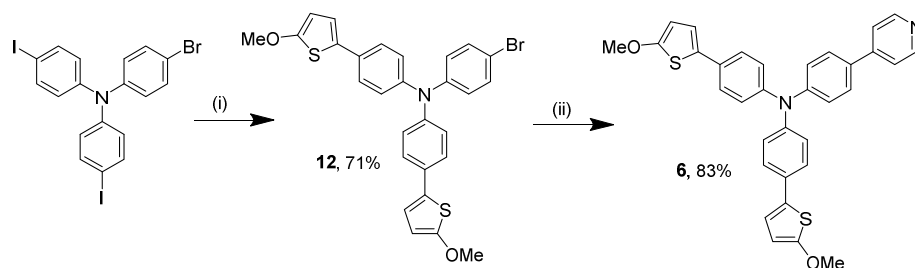
The grafting of two carbazole fragments onto the triphenylamine core by a copper-catalyzed reaction with either 4-bromo-4',4''-diiodotriphenylamine or 4,4',4''-triiodotriphenylamine led to the bromo- and iodo-derivatives **10** and **11**, respectively. These compounds were readily converted into chromophores **4** and **5** in moderate yield by Suzuki–Miyaura cross-coupling

with pyridin-4-ylboronic acid or Heck cross-coupling with 4-vinylpyridine, respectively (Scheme 2).



Scheme 2. (i) carbazole, 1,10-phenanthroline, CuI, Cs₂CO₃, DMF, 18 h, 200 °C (ii) pyridin-4-ylboronic acid, PdCl₂(PPh₃)₂, Na₂CO₃, dioxane/H₂O 4:1, Δ, 18 h (iii) 4-vinylpyridine, Pd(OAc)₂, P(*o*-tol)₃, diethylamine, DMF, 90 °C, 24 h.

Finally, compound **6** was prepared in two steps from 4-bromo-4',4''-diiodotriphenylamine. An initial double Suzuki–Miyaura cross-coupling reaction with 2-(4,4,5,5-tetramethyl-1,3,2-dioxaborolan-2-yl)-5-methoxythiophene gave intermediate **12**, which after a second Suzuki–Miyaura reaction with pyridin-4-ylboronic acid led to the desired compound **6** in good yield (Scheme 3).



Scheme 3. (i) 2-(4,4,5,5-tetramethyl-1,3,2-dioxaborolan-2-yl)-5-methoxythiophene, PdCl₂(PPh₃)₂, Na₂CO₃, 1,4-dioxane/H₂O 4:1, Δ, 18 h (ii) pyridin-4-ylboronic acid, PdCl₂(PPh₃)₂, Na₂CO₃, dioxane/H₂O 4:1, Δ, 18 h.

Photophysical properties. The UV/Vis and photoluminescence (PL) spectroscopic data for compounds **1–6** measured in CHCl₃ at room temperature are presented in Table 1. The analyses were carried out using low concentrations of chromophores ($0.5\text{--}1.5 \times 10^{-5}$ M). To facilitate comparison of the photophysical properties, the results for unsubstituted triphenylamine analogs **A–C** are also included in Table 1. As representative examples, the spectra of compounds **1**, **4** and **6** are provided in Figure 2. Compounds **1–6** exhibit blue-green emission with quantum yields between 0.31 and 0.80. In all cases, a significant red shift in the emission maximum was observed in comparison to the unsubstituted analogs **A–C**. It can be seen from Figure 2 that the absorption maxima of **1**, **4** and **6** depend on the electron-donating substituent and the value increases in the following order: 9*H*-carbazol-9-yl (**4**) < methoxy (**1**) < 5-methoxythiophen-2-yl (**6**). As far as the emission is concerned, the 9*H*-carbazol-9-yl derivative **4** is also the most strongly blue-shifted whereas the methoxy- and 5-methoxythiophen-2-yl- derivatives **1** and **6** exhibit similar emission maxima at $\lambda_{\text{max}} = 511$ nm. As observed for compounds **A–C** and other families of chromophores,^{9b,25} absorption and emission increase when an acetylenic linker is placed between the triphenylamine fragment and the pyridine moiety and an even more remarkable increase is observed when a vinylic linker is incorporated [in the methoxy series λ_{max} (**1**) < λ_{max} (**3**) < λ_{max} (**2**) and in the carbazole series λ_{max} (**4**) < λ_{max} (**5**)]. Compounds **1–6** exhibit red-shifted absorption in the presence of

camphorsulfonic acid due to protonation of the pyridine ring, which enhances the ICT. Nevertheless, in contrast to unsubstituted triphenylamine derivatives **A–C**, the protonated forms of **1–6** are not emissive.

Table 1. UV/Vis and PL data in CHCl₃.

Compd ^a	UV/vis λ_{max} , nm (ϵ , mM ⁻¹ ·cm ⁻¹)	UV/vis λ_{max} , nm ^b (ϵ , mM ⁻¹ ·cm ⁻¹)	PL λ_{max} , nm	Φ_F^c	Stokes shift cm ⁻¹
1	352 (26.6)	430 (39.0)	511	0.60	8840
2	399 (38.1)	485 (41.5)	533	0.48	6301
3	371 (36.5)	460 (37.9)	521	0.52	7760
4	341 (50.1)	429 (32.4)	473	0.44	8184
5	387 (36.9)	468 (41.9)	510	0.80	6231
6	368 (68.5)	445 (35.9)	511	0.31	7604
A ²³	349 (25.6)	416 (28.9)	444	0.50	6130
B ²³	386 (28.0)	467 (27.5)	485	0.45	5288
C ²³	370 ((31.0)	449 (31.0)	456	0.78	5097

^a All spectra were recorded at room temperature at $c = 0.5 \times 10^{-5}$ to 1.5×10^{-5} M. ^b Data in the presence of 10^{-2} M camphorsulfonic acid. ^c Fluorescence quantum yield ($\pm 10\%$) determined relative to 9,10-bis-phenylethynylantracene in cyclohexane ($\Phi_F = 1.00$).²⁶

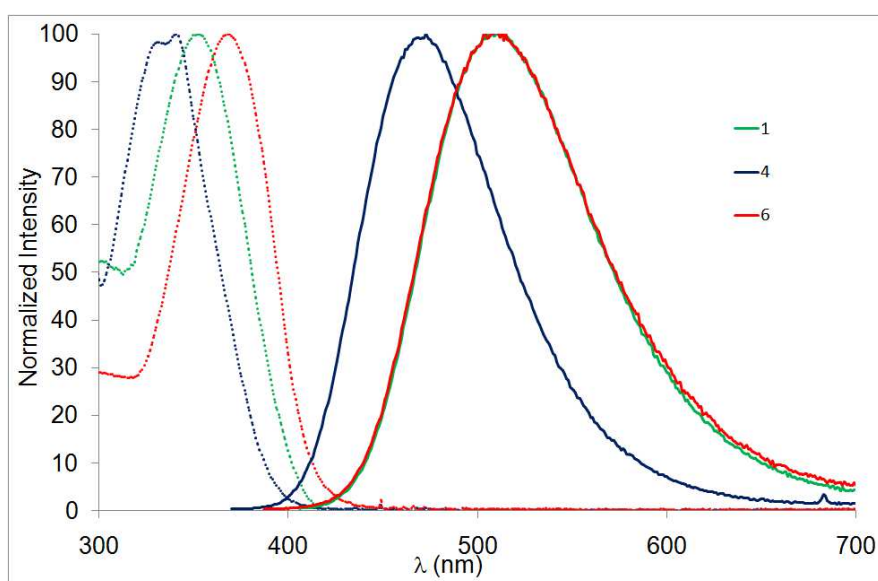


Figure 2. Normalized absorption (dashed lines) and emission spectra (solid lines) of compounds **1**, **4** and **6** in CHCl₃ solution.

Emission solvatochromic studies were performed in an effort to gain an insight into the photophysical processes of these new push-pull molecules. Thus, the emission spectra of compounds **1–6** were recorded in a series of aprotic solvents of different polarity (Table 2, Figure 3). As expected for emissive push-pull derivatives,^{9b, 27} strong positive solvatochromism was observed on increasing the polarity, as estimated by the Dimroth–Reichardt scale.²⁸ For each compound the emission maximum was plotted *versus* the Dimroth–Reichardt polarity parameter (Figure S40, see Supporting Information) and in all cases good linearity was obtained. The slope of the corresponding regression line (SP) allows an evaluation of the ICT into the chromophores. As expected, the highest SP values were obtained for compounds **2** and **3**, which exhibit the most red-shifted absorption and emission in CHCl₃. Compounds **1–3**, **5** and **6** have higher SP values than their unsubstituted analogs. Surprisingly, compound **4** has a lower SP value than **A**, thus confirming that the carbazole fragments on the triphenylamino core have a significantly weaker influence on the ICT than the two other substituents evaluated (methoxy and 5-methoxythiophen-2-yl).

Table 2. Emission solvatochromism in various aprotic solvents.

Compd	Heptane 30.9 ^a λ_{\max} , nm	Toluene 33.9 ^a λ_{\max} , nm	1,4-Dioxane 36.0 ^a λ_{\max} , nm	THF 37.4 ^a λ_{\max} , nm	CH ₂ Cl ₂ 40.7 ^a λ_{\max} , nm	Acetone 42.2 ^a λ_{\max} , nm	MeCN 45.6 ^a λ_{\max} , nm	SP ^b
1	451	475	477	508	523	536	554	7.22
2	468	500	511	556	574	590	607	9.94
3	460	480	484	522	540	560	605	9.91
4	426	443	444	466	476	487	504	5.37
5	455	471	478	509	524	536	555	7.19
6	454	469	473	496	519	532	552	7.08
A ²³	389	412	-	433	451	458	472	5.60
B ²³	424	448	-	475	498	500	515	6.38
C ²³	398	421	-	450	473	481	497	7.11

^a E_T(30), Dimroth–Reichardt polarity parameter in kcal mol⁻¹. ^b Slope of the regression line λ_{\max} (nm) *versus* E_T(30) in nm mol kcal⁻¹.

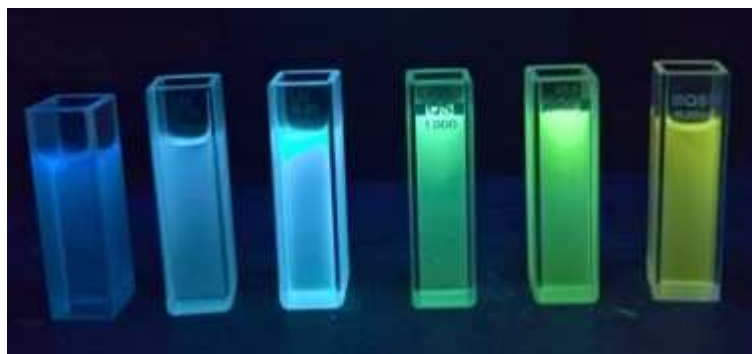


Figure 3. Fluorescence color changes for **5** in various solvents (from left to right: *n*-heptane, toluene, 1,4-dioxane, CHCl_3 , CH_2Cl_2 and MeCN). Photographs were taken in the dark upon irradiation with a hand-held UV lamp ($\lambda_{\text{em}} = 366 \text{ nm}$).

Electrochemical properties. The redox properties of the push-pull molecules **1–6** were studied by cyclic voltammetry (CV) in DMF, using NBu_4PF_6 (0.1M) as the supporting electrolyte in a three-electrode cell (working electrode: glassy carbon; counter electrode: Pt; reference: Ag wire). All measurements were obtained using Fc^+/Fc as the internal reference. The potential values are given vs. saturated calomel electrode (SCE)²⁹ for comparison with unsubstituted triphenylamine molecules **A–C**²³ (Table 3). The cyclic voltammograms are presented in Figure 4.

Table 3. Electrochemical data,^a E_{HOMO} and E_{LUMO} values.^b

Compd	E^{ox} (V)	E^{red} (V)	ΔE (eV)	E_{HOMO} (eV)	E_{LUMO} (eV)
1	0.79 ^c	-2.26 ^c	3.04	-5.14	-2.09
2	0.75 ^c	-2.02 ^d	2.76	-5.10	-2.33
3	0.79 ^c	-2.08 ^d	2.88	-5.14	-2.27
4	0.99 ^d	-2.34 ^e	3.33	-5.34	-2.00
5	0.94 ^e	-1.92 ^d	2.87	-5.29	-2.42
6	0.77 ^c	-2.31 ^c	3.08	-5.12	-2.04
A ²³	1.07	-2.15	3.22	-5.42	-2.20
B ²³	1.06	-1.82	2.87	-5.41	-2.54
C ²³	1.09	-1.96	3.05	-5.44	-2.40

^a Potentials are given vs. SCE, glassy carbon working electrode, Pt counter electrode, 20 °C in DMF, 0.1M NBu_4PF_6 as supporting electrolyte, 100 mV s^{-1} scan rate. Ferrocene was used as internal reference ($E_{1/2} = +0.44 \text{ V}$ vs. SCE). ^b E_{HOMO} , E_{LUMO} were determined empirically from the oxidation and reduction potentials according to the empirical relationship $E_{\text{HOMO}} = -(E^{\text{ox}} + 4.35) \text{ eV}$; $E_{\text{LUMO}} = -(E^{\text{red}} + 4.35) \text{ eV}$. ^c $E_{1/2}$. ^d Quasi-reversible. ^e Irreversible.

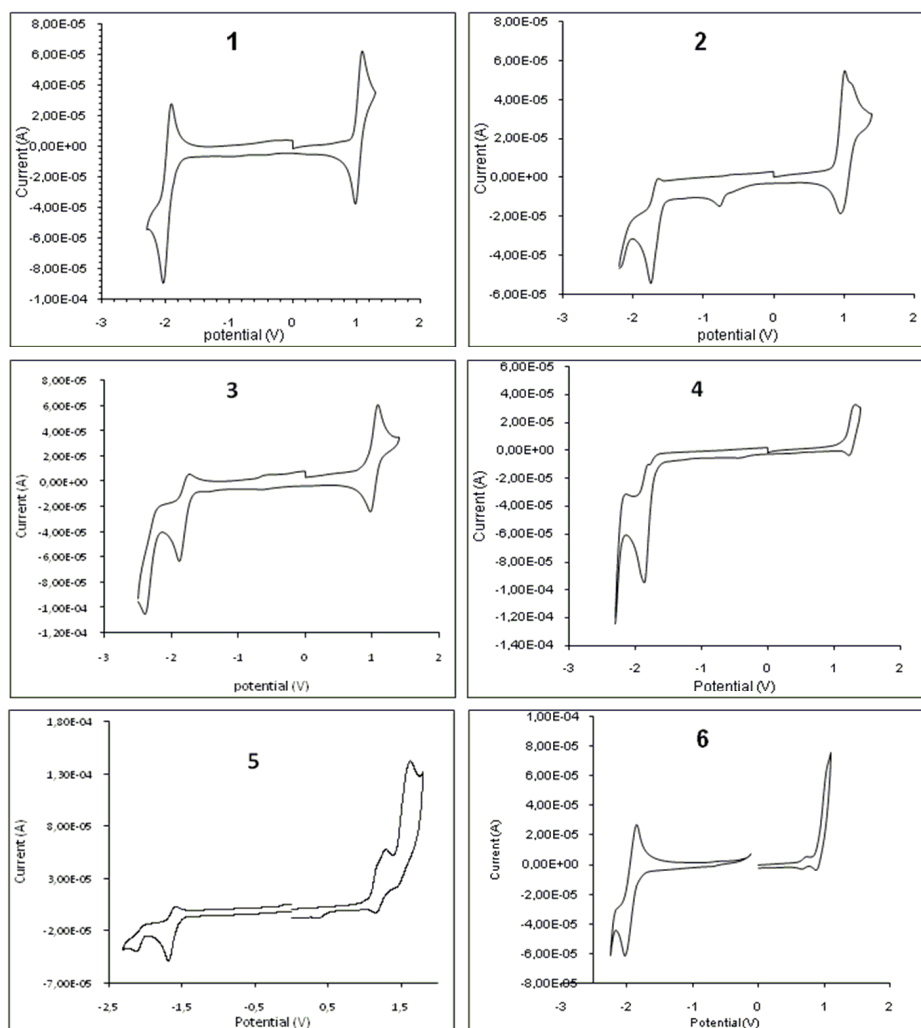


Figure 4. Cyclic voltammograms of compounds **1–6** with NBu_4PF_6 as the supporting electrolyte, measured in DMF (working electrode: glassy carbon; counter electrode: Pt; reference: Ag wire), 100 mV s^{-1} scan rate.

Compounds **1–6** all exhibited one or several oxidation processes. Molecules **1–3**, which bear 4-methoxy substituents on two phenyl groups of the triphenylamine moiety, showed a first reversible redox process ($E_{1/2} = +0.75/+0.79 \text{ V}$) that became quasi-reversible for carbazole derivatives **4–5** and irreversible for compound **6**, which contains methoxythiophene branches, at a scan rate of 100 mV s^{-1} . The potential values for the first oxidation waves of **4** ($E_{1/2}^{\text{ox}} = +0.99 \text{ V}$) and **5** ($E_p^{\text{ox}} = +0.94 \text{ V}$), which bear carbazole substituents, are higher than those for compounds **1–3** and **6** but approach the values obtained for **A**, **B** and **C**.²³ The lower oxidation potentials obtained for **1–3** can be explained by the increase in the electron-donating effect of the triphenylamine containing methoxy groups. Incorporation of a thienyl ring in compound **6**

did not affect the potential value (when compared to **1**). Finally, the incorporation of carbazole units only has a weak influence on the electron-donating character of the substituted triphenylamine.

Compounds **1** and **6** exhibited a first reversible reduction process on scanning from 0 to -2.5 V, whereas the process was quasi-reversible for compounds **2**, **3** and **5**. A loss of reversibility was observed for **4**. Potential values ($E_{1/2}^{\text{red}}$ or E_p^{red}) were in the range from -1.92 V to -2.34 V vs. SCE. As reported previously for molecules **A–C**, compounds bearing an acetylenic or vinylic π -linker are reduced at more positive potentials. The same trend was observed for the carbazole derivatives **4** and **5**. These results show that the reduction of the pyridine moiety is easier after the incorporation of either an acetylenic or vinylic π -linker.

The values of the E_{HOMO} , E_{LUMO} and the energy band gap (ΔE) were estimated for all molecules from the experimental E^{ox} and E^{red} potentials by the empirical relationship $E_{\text{HOMO}} = -(E^{\text{ox}} + 4.35)$ eV; $E_{\text{LUMO}} = -(E^{\text{red}} + 4.35)$ eV (Table 3). The results indicate that the 4-methoxytriphenylamine derivatives **1–3** have a lower energy gap in comparison to molecules **A–C**. Furthermore, the energy gap remained almost unchanged on incorporating a thienyl group (in **6**) between the methoxy substituent and the phenyl groups of the triphenylamine. Also, the HOMO-LUMO overlap values obtained for chromophores **4** and **5** in comparison with molecules **A** and **C** confirm the weak effect of donor modification by grafting a carbazole moiety. The trends outlined above are consistent with the variations in λ_{max} of the charge transfer bands observed in the electronic spectra of compounds **1–6**. Contrary to most cases, the estimated electrochemical gap of **4** (3.33 eV) is greater than that for **A** (3.22 eV). However, this is also consistent with the λ_{max} measurements obtained from the electronic spectra: the maximum wavelength for **4** is lower (341 nm) than that for **A** (349 nm).

Thermal properties. The thermal behavior of compounds **1–6** was studied by differential scanning calorimetry (DSC). The thermographs are shown in Figures S33–S38 of the

Supporting Information, while the melting points (T_m) and thermal decomposition temperatures (T_d) are listed in Table 4.

Table 4. Thermal properties of compounds **1–6**.

Compd	1	2	3	4	5	6
T_m (°C)	155	-	-	-	249	-
T_d (°C)	330	285	285	300	260	200

Only chromophores **1** and **5** exhibited an endothermic peak due to melting. All of the other compounds decomposed directly without melting. Carbazole derivative **5**, with an embedded ethenylene spacer, was not stable in the liquid state ($T_m = 249$ °C). This compound gradually decomposed upon continued heating above its melting point. Loss of residual water was also observed for **5** up to 120 °C. This finding is in contrast with the methoxy derivative **1**, which contains an unextended π -linker, which was stable in the liquid phase for a further 175 °C above its melting point. Structural analogs **2** and **3**, which differ only in the π -spacer (double or triple bond), exhibited almost identical thermal behavior, with a decomposition temperature estimated at $T_d = 285$ °C. Similar DSC curves were also recorded for molecules **4** and **6**, for which a broad endothermic peak due to the enantiotropic solid-solid transition was detected at 150 °C and 90 °C, respectively. This transition was immediately followed by a second undefined endothermic phenomenon and subsequent exothermic decomposition for both chromophores.

The gradual elongation of the π -spacer in the methoxy analogs **1/2/3** led to a reduction in the thermal stability (none/ethenylene/acetylene spacer $\rightarrow T_d = 330/285/285$ °C). An analogous effect was also observed for the carbazole derivatives **4/5** (none/ethenylene spacer $\rightarrow T_d = 300/260$ °C). The lowest T_d value was determined for compound **6**, which contained methoxythiophene donors. In general, the enlargement of the π -linker seemed to decrease the thermal robustness of the compounds under investigation. Regarding the variation of the

donors, this structural modification increased the thermal stability in the order 5-methoxythien-2-yl \rightarrow *N*-carbazole \rightarrow methoxy group.

DFT calculations. The Gaussian W09 package³⁰ was employed to investigate the spatial and electronic properties of chromophores **1–6** at the DFT level. The initial geometries of the molecules **1–6** were estimated and optimized using the DFT B3LYP/6-31G(d) and DFT B3LYP/6-311G(d,p) methods. The HOMO and LUMO energies, their differences, and the ground state dipole moments were calculated at the DFT B3LYP/6-311++G(d,f,p) level and the results are summarized in Table 5.

Table 5. DFT calculated properties of chromophores

Compd	Symmetry group	E_{HOMO} (eV)	E_{LUMO} (eV)	ΔE (eV)	μ (D)
1	C2	-5.13 ^a	-1.41 ^a	3.72	4.1
2	C1	-5.07 ^a	-1.91 ^a	3.16	5.3
3	C2	-5.16 ^a	-1.80 ^a	3.36	5.5
4	C2	-5.54 ^a	-1.83 ^a	3.71	1.6
5	C1	-5.46 ^a	-2.25 ^a	3.21	2.1
6	C2	-5.03 ^a	-1.60 ^a	3.43	2.8
A ²³	C2	-5.44 ^b	-1.57 ^b	3.88	3.8
B ²³	C1	-5.36 ^b	-2.05 ^b	3.30	4.8
C ²³	C2	-5.45 ^b	-1.94 ^b	3.51	5.0

^a Calculated at the DFT B3LYP/6-311++G(d,f,p) level. ^b Calculated at the DFT B3LYP/6-311++G(2d,p) level.

The calculated energies of the HOMO and LUMO of pyridine derivatives **1–6** ranged from -5.54 to -5.03 and from -2.25 to -1.41 eV, respectively. It is clear that the calculated $E_{\text{HOMO/LUMO}}$ values reflect structural differences between the individual chromophores and show a close correlation with the electrochemical data (Figure 5). The electron-donating ability of methoxy, carbazole and methoxythiophene moieties, the nature of the π -linker, and the electron-withdrawing character of the pyridine ring all have a significant effect on the calculated HOMO-LUMO gaps (ΔE). The calculated gaps, which are within the range $\Delta E = 3.72\text{--}3.16$ eV, correlate well with the electrochemical data, with differences not exceeding

0.68 eV. The calculated HOMO-LUMO gaps for the linear chromophores **1–3** resemble those obtained for unsubstituted triphenylamine derivatives **A–C**.²³ The largest ΔE values (3.72 and 3.88 eV) were calculated for compounds **1** and **A** (without a spacer), whereas the narrowest gaps of 3.16 and 3.30 eV were computed for compounds **2** and **B**, which contain a vinyl spacer. It can also be seen that the introduction of two electron donors on the central triphenylamine core reduced the HOMO-LUMO gaps when compared to the parent derivatives **A–C** (Figure 5). The calculated ΔE values are almost identical for the methoxy and carbazole derivatives. On the other hand, for methoxythienyl derivative **6** the ΔE value is significantly lower. The HOMO/LUMO localizations are represented in Figure 6. The HOMO is located either on the central amino donor atom (**1–5**), the carbazole (**4** and **5**) or the phenylene units bearing the methoxythiophene substituents (**6**). On the other hand, the LUMO occupies the pyridine acceptor and the adjacent π -system. Hence, all molecules **1–6** can be considered as charge-transfer chromophores. The calculated ground state dipole moments reflect the molecular structures and symmetry. Chromophores **4–6** bear bulky carbazole and methoxythiophene groups and these showed low dipole moments of 1.6–2.8 D, whereas methoxy derivatives **1–3** have dipole moments in the range 4.1 to 5.5 D.

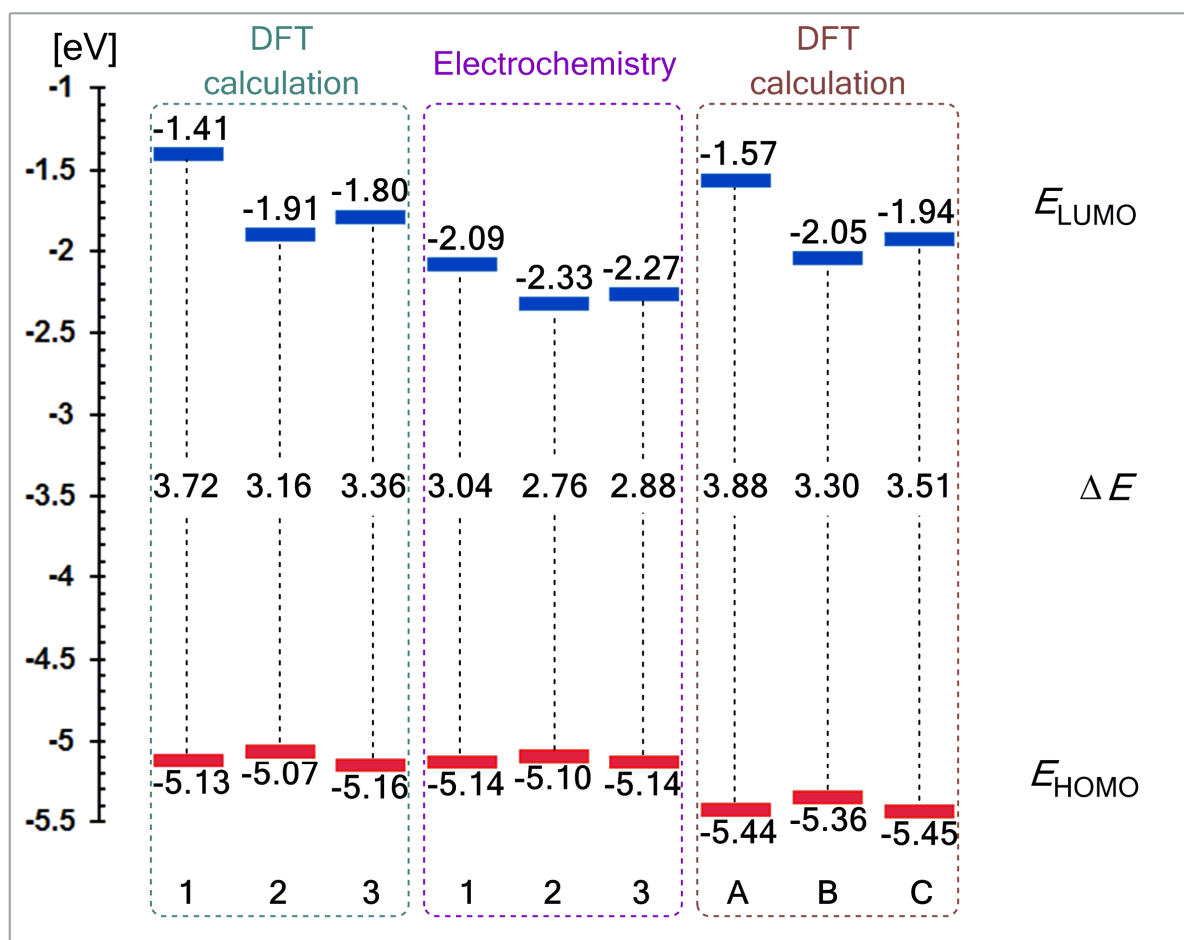


Figure 5. Energy level diagram for linear chromophores **1–3** and **A–B**.

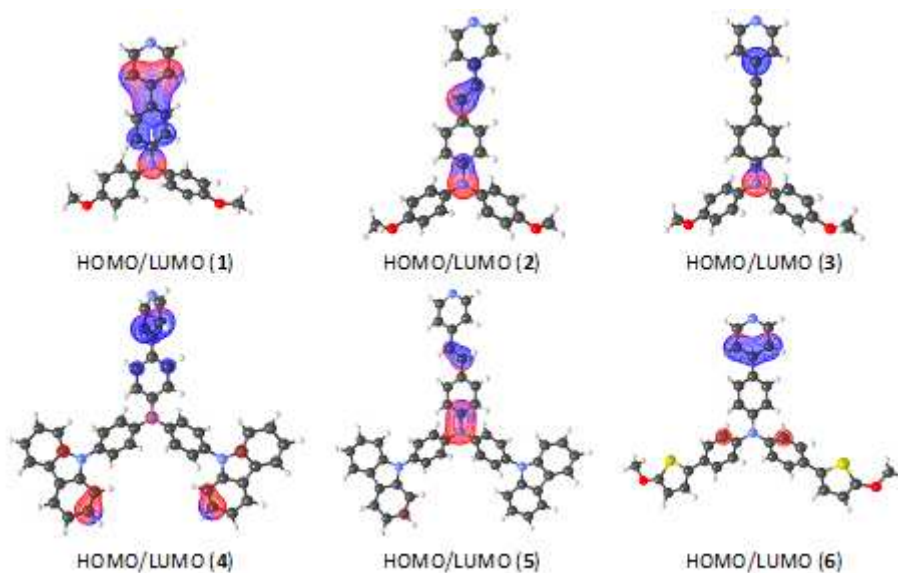


Figure 6. Representative HOMO (red) and LUMO (blue) localizations in **1–6**.

3. Conclusions

A series of push-pull derivatives has been designed with a pyridine electron-withdrawing fragment and methoxy-, 9*H*-carbazol-9-yl- and 5-methoxythiophen-2-yl-substituted diphenylamino groups as electron-donating units. The reinforcement of the electron-donating character of the diphenylamino group leads to enhanced ICT into the push-pull structure with respect to their unsubstituted diphenylamino derivatives, as demonstrated by spectroscopic and electrochemical measurements as well as by DFT calculations. This enhanced ICT also explains the emission quenching observed for compounds **1–6** upon protonation in contrast to the results observed for **A–C**.²³

4. Experimental section

General: All reactions were carried out in vacuum-dried Schlenk flasks under Ar. All compounds and solvents were purchased from Aldrich or TCI and were used without further purification, except for tetrahydrofuran, which was freshly distilled from Na/benzophenone ketyl. 4-Iodopyridine³¹ and 4-bromo-*N,N*-bis(4-iodophenyl)aniline^{19b} were obtained according to reported procedures. Column chromatography was carried out using silica gel 60 (particle size 0.040–0.063 mm, 230–400 mesh; Merck) and commercially available solvents. Thin-layer chromatography (TLC) was conducted on aluminium sheets coated with silica gel 60 F254 and compounds were visualized with a UV lamp (254 or 360 nm). ¹H and ¹³C NMR spectra were recorded in CDCl₃ at 500 MHz and 125 MHz, respectively, at 25 °C on a Bruker AscendTM instrument, using the appropriate solvent signal (CDCl₃ 7.25 and 77.23 ppm) as internal reference. The apparent resonance multiplicities are described as s (singlet), d (doublet), t (triplet) and m (multiplet). High-resolution MALDI mass spectra were measured on an LTQ Orbitrap XL MALDI mass spectrometer (Thermo Fisher Scientific, Bremen, Germany) equipped with a nitrogen UV laser (337 nm, 60 Hz). The LTQ Orbitrap instrument

was operated in positive-ion mode over a normal mass range (m/z 50–2000) with a resolution of 100,000 at $m/z = 400$. 2,5-Dihydroxybenzoic acid (DHB) was used as a matrix. Thermal properties were measured by differential scanning calorimetry DSC on a Mettler-Toledo STARe System DSC 2/700 equipped with an FRS 6 ceramic sensor and HUBER TC100-MT RC 23 cooling system in open aluminum crucibles under an N₂ atmosphere. DSC curves were obtained at a scanning rate of 3 °C min⁻¹.

DFT calculations: HOMO/LUMO localizations in **1–6** were derived from the calculations using the Gaussian W09 package at the DFT level. Geometries for visualizations were optimized using the DFT B3LYP/311G method and are visualized as red-HOMO localization and blue-LUMO localization. The visualizations were generated in the program OPchem.³²

4-Iodo-*N,N*-bis(4-methoxyphenyl)aniline (7): In a Schlenk tube under an inert atmosphere of argon, 4'-bromo-*N,N*-bis(4-methoxyphenyl)aniline (1.31 g, 3.42 mmol) was dissolved in anhydrous THF (30 mL). The resulting solution was cooled to -78 °C and *n*-BuLi (1.51 mL, 2.5 M solution in hexanes, 3.764 mmol) was added dropwise. The reaction mixture was stirred at -78 °C for 30 min and iodine (0.869 g, 3.42 mmol) in anhydrous THF (5 mL) was added dropwise. The resulting mixture was slowly warmed and stirred for 3 h. Solvents were removed under reduced pressure and the mixture was diluted with CH₂Cl₂ (50 mL) and saturated aqueous solution of NH₄Cl (70 mL). The aqueous layer was washed with CH₂Cl₂ (2 × 30 mL). The combined organic layers were washed with brine (50 mL) and dried with Na₂SO₄. After removal of the solvent under reduced pressure, the residue was purified by flash chromatography (SiO₂, CH₂Cl₂/hexane 1:2) and subsequent recrystallization from boiling ethanol to give compound **7** as a colorless solid (0.864 g, 2.00 mmol, 59%). ¹H NMR (400 MHz, CDCl₃): $\delta = 3.79$ (s, 6H), 6.66–6.83 (m, 2H), 6.80–6.84 (m, 4H), 7.01–7.03 (m, 4H), 7.39–7.41 (m, 2H). HRMS (MALDI) m/z calcd. for C₂₀H₁₈INO₂: 595.0131 [M⁺], found 595.0144. The spectroscopic data are consistent with those reported in the literature.³³

4-Methoxy-*N*-(4-methoxyphenyl)-*N*-{4-[(trimethylsilyl)ethynyl]phenyl}aniline (8): In a Schlenk tube under an inert atmosphere of argon, *N,N*-bis(4-methoxyphenyl)-4'-iodoaniline (394 mg, 0.914 mmol), trimethylsilylacetylene (152 μ L, 1.10 mmol), CuI (4 mg, 0.021 mmol) and PdCl₂(PPh₃)₂ (32 mg, 0.046 mmol) were dissolved in anhydrous diisopropylamine (25 mL). The resulting solution was stirred at 60 °C for 1 h. The mixture was cooled and diisopropylamine was removed under reduced pressure. The mixture was diluted with diethyl ether (50 mL) and water (70 mL). The aqueous layer was washed with diethyl ether (2 \times 30 mL). The combined organic layers were washed with brine (50 mL) and dried with Na₂SO₄. After removal of the solvent under reduced pressure, the residue was purified by column chromatography (SiO₂, CH₂Cl₂/hexane 1:2) to give compound **8** as a yellow oil (350 mg, 0.872 mmol, 95% yield). ¹H NMR (400 MHz, CDCl₃): δ = 0.24 (s, 9H), 3.78 (s, 6H), 6.77–6.84 (m, 6H), 7.05–7.08 (m, 4H), 7.25–7.23 (m, 2H). EI-MS (70 eV) *m/z* (rel. int.): 401 (M⁺, 100), 386 (40), 193 (10). The spectroscopic data are consistent with those reported in the literature.³⁴

4-Ethynyl-*N,N*-bis(4-methoxyphenyl)aniline (9): In a round-bottomed flask *N,N*-bis(4-methoxyphenyl)-4'-(trimethylsilylethynyl)aniline (350 mg, 0.872 mol) and K₂CO₃ (311 mg, 1.31 mol) were dissolved in methanol (50 mL). The reaction mixture was stirred for 18 h at room temperature. The methanol was removed under reduced pressure and the mixture was diluted with CH₂Cl₂ (50 mL) and water (100 mL). The aqueous layer was washed with CH₂Cl₂ (2 \times 30 mL), brine (50 mL) and dried with Na₂SO₄. After removal of the solvent under reduced pressure, the residue was purified by column chromatography (SiO₂, CH₂Cl₂/hexane 1:2) to give compound **9** as a yellow oil (232 g, 0.704 mmol, 60%). ¹H NMR (400 MHz, CDCl₃): δ = 3.01 (s, 1H), 3.76 (s, 6H), 6.77–6.84 (m, 6H), 7.01–7.05 (m, 4H), 7.23–7.25 (m, 2H). EI-MS (70 eV) *m/z* (rel. int.): 329 (M⁺, 100), 314 (70). The spectroscopic data are consistent with those reported in the literature.³¹

***N,N*-Bis[4-(9H-carbazol-9-yl)phenyl]-4-bromoaniline (10):** In a glass autoclave 4'-bromo-*N,N*-bis(4-iodophenyl)aniline (210 mg, 0.365 mmol), carbazole (152 mg, 0.909 mmol), 1,10-phenanthroline (120 mg, 0.666 mmol), CuI (60 mg, 0.315 mmol) and Cs₂CO₃ (490 mg, 1.50 mmol) were dissolved in dry DMF and argon was bubbled through for 5 min. The reaction mixture was stirred at 200 °C for 18 h. The resulting mixture was cooled and the DMF was removed under reduced pressure. Saturated aqueous NaHCO₃ (70 mL) was added and the mixture was extracted with CH₂Cl₂ (3 × 50 mL). The organic layer was washed with brine (70 mL) and dried with Na₂SO₄. After removal of the solvent under reduced pressure, the residue was purified by column chromatography (SiO₂, CH₂Cl₂/hexane 1:2) to give compound **10** as a colorless solid (86 mg, 0.131 mmol, 36%). ¹H NMR (400 MHz, CDCl₃): δ = 7.18–7.20 (m, 2H), 7.28–7.31 (m, 4H), 7.36–7.38 (m, 4H), 7.41–7.50 (m, 14H), 8.15 (d, *J* = 7.5 Hz, 4H). HRMS (MALDI) *m/z* calcd. for C₄₂H₂₈BrN₃: 653.1461 [M⁺], found 653.1473. The spectroscopic data are consistent with those reported in the literature.^{20a}

***N,N*-Bis[4-(9H-carbazol-9-yl)phenyl]-4-iodoaniline (11):** This compound was obtained from tris(4-iodophenyl)amine (623 mg, 1 mmol) and carbazole (335 mg, 2 mmol) by the same procedure as described for **10**. The crude product was purified by column chromatography (SiO₂; petroleum ether:CH₂Cl₂, 4:1). Colorless solid (217 mg, 31%). ¹H NMR (300 MHz, CDCl₃): δ = 7.07–7.10 (m, 2H), 7.28–7.53 (m, 20H), 7.67–7.70 (m, 2H), 8.15–8.18 (m, 4H) ppm. ¹³C NMR (75 MHz, CDCl₃): δ = 86.8, 109.9, 120.1, 120.5, 123.5, 125.3, 126.1, 126.6, 128.3, 132.9, 138.8, 141.1, 146.3, 147.3 ppm. HRMS (MALDI) *m/z* calcd. for C₄₂H₂₈IN₃: 701.1322 [M⁺], found 701.1319.

4-Bromo-*N,N*-bis[4-(5-methoxythiophen-2-yl)phenyl]aniline (12): In a Schlenk tube under an inert atmosphere of argon, 4'-bromo-*N,N*-bis(4-iodophenyl)aniline (218 mg, 0.379 mmol), 2-(4,4,5,5-tetramethyl-1,3,2-dioxaborolan-2-yl)-5-methoxythiophene (200 mg, 0.833 mmol), and Na₂CO₃ (80 mg, 0.755 mmol) were dissolved in dioxane/water 4:1 (25 mL) and argon

was bubbled through for 5 min, followed by the addition of PdCl₂(PPh₃)₂ (11 mg, 0.016 mmol). The reaction mixture was stirred at 90 °C for 18 h. The mixture was then cooled and the solvents were removed under reduced pressure. The residue was diluted with CH₂Cl₂ (50 mL) and water (70 mL). The aqueous layer was extracted with CH₂Cl₂ (2 × 30 mL). The combined organic layers were washed with brine (50 mL) and dried with Na₂SO₄. After removal of the solvent under reduced pressure, the residue was purified by column chromatography (SiO₂, CH₂Cl₂/hexane 1:2) to give compound **12** as an orange solid (148 mg, 0.270 mmol, 71%). ¹H NMR (500 MHz, CDCl₃): δ = 3.90 (s, 6H), 6.16 (d, *J* = 3.9 Hz, 2H), 6.86 (d, *J* = 3.9 Hz, 2H), 6.96–6.98 (m, 2H), 7.02–7.04 (m, 4H), 7.32–7.36 (m, 6H) ppm. ¹³C NMR (100 MHz, CDCl₃): δ = 60.4, 104.9, 115.3, 120.2, 124.7, 125.4, 126.0, 130.0, 130.1, 132.5, 145.8, 146.7, 165.8 ppm. HRMS (MALDI) *m/z* calcd. for C₂₈H₂₂BrNO₂S₂: 547.0270 [M⁺], found 547.0278.

General Procedure for the Suzuki–Miyaura cross-coupling: In a Schlenk tube under an inert atmosphere of argon, the appropriate TPA bromide (1.0 equiv.), pyridine-4-boronic acid (1.2 equiv.) and Na₂CO₃ (1.0 equiv.) were dissolved in dioxane/water 4:1 (25 mL) and argon was bubbled through for 5 min, followed by the addition of PdCl₂(PPh₃)₂ (0.05 equiv.). The resulting solution was stirred at 90 °C for 18 h. The mixture was then cooled and the solvents were removed under reduced pressure. The residue was diluted with CH₂Cl₂ (50 mL) and water (70 mL). The aqueous layer was washed with CH₂Cl₂ (2 × 30 mL). The combined organic layers were washed with brine (50 mL) and dried with Na₂SO₄. After removal of the solvent under reduced pressure, the residue was purified by column chromatography (SiO₂, CHCl₃/ethyl acetate 1:1).

General Procedure for the Heck cross-coupling: Palladium acetate (10%) and tris-*o*-tolylphosphine (20%) were introduced into a dry and degassed NEt₃/DMF (9 mL, 2:1, v/v) mixture, which was stirred for 15 min. The mixture was degassed again by gentle bubbling of

nitrogen. The appropriate halogen derivative (1.0 equiv.) and vinylpyridine (1.3 eq.) were added. The mixture was then stirred at 85–90 °C under nitrogen for 3 h. After cooling, the NEt₃ was removed under vacuum. The crude mixture was diluted with CH₂Cl₂ and washed with water and saturated NaHCO₃. After removal of the solvent under reduced pressure, the residue was purified by column chromatography (SiO₂).

4-Methoxy-N-(4-methoxyphenyl)-N-[4-(pyridin-4-yl)phenyl]aniline (1): This compound was prepared according to the general procedure for the Suzuki–Miyaura cross-coupling starting from 4-bromo-*N,N*-bis(4-methoxyphenyl)aniline (200 mg, 0.521 mmol). Purification by column chromatography afforded the pure chromophore **1** as a yellow solid (156 mg, 0.406 mmol, 78%). ¹H NMR (500 MHz, CDCl₃): δ = 3.80 (s, 6H), 6.82–6.86 (m, 4H), 6.96–6.97 (m, 2H), 7.08–7.10 (m, 4H), 7.43–7.46 (m, 4H), 8.56–8.57 (m, 2H) ppm. ¹³C NMR (125 MHz, CDCl₃): δ = 55.7, 115.0, 119.9, 120.8, 127.3, 127.6, 129.0, 140.4, 147.94, 150.0, 150.3, 156.5 ppm. HRMS (MALDI) *m/z* calcd. for C₂₅H₂₂N₂O₂: 382.1676 [M⁺], found 382.1681. The spectroscopic data are consistent with those reported in the literature.³⁵

(E)-4-Methoxy-N-(4-methoxyphenyl)-N-[4-[2-(pyridin-4-yl)vinyl]phenyl]aniline (2): This compound was prepared according to general procedure for the Heck cross-coupling starting from 4-bromo-*N,N*-bis(4-methoxyphenyl)aniline (300 mg, 0.78 mmol, 1 equiv.) and 4-vinylpyridine (107 mg, 1.02 mmol, 1.3 equiv). The crude product was purified by column chromatography (SiO₂; ethyl acetate/petroleum ether 1:1). Yellow solid (188 mg, 59%). ¹H NMR (300 MHz, CDCl₃): δ = 3.80 (s, 6H), 6.79–7.90 (m, 7H), 7.08 (d, *J* = 6.9 Hz, 4H), 7.22 (d, *J* = 16.5 Hz, 1H), 7.34–7.30 (m, 4H) 8.52 (d, *J* = 6.0 Hz, 2H) ppm. ¹³C NMR (75 MHz, CDCl₃): δ = 55.5, 114.8, 119.7, 120.5, 122.8, 127.0, 127.9 (2C), 132.9, 140.3, 145.2, 149.4, 150.1, 156.3 ppm. HRMS (MALDI) *m/z* calcd. for C₂₇H₂₅N₂O₂: 409.1910 [M + H⁺], found 409.1910.

4-Methoxy-*N*-(4-methoxyphenyl)-*N*-[4-(pyridin-4-ylethynyl)phenyl]aniline (3): In a Schlenk tube under an inert atmosphere of argon, *N,N*-bis(4-methoxyphenyl)-4'-(ethynyl)aniline (232 mg, 0.704 mmol), 4-iodopyridine (159 mg, 0.776 mmol) and CuI (3 mg, 0.016 mmol) were dissolved in anhydrous dioxane/trimethylamine 4:1 (25 mL) and argon was bubbled through for 5 min, followed by the addition of Pd(PPh₃)₄ (16 mg, 0.014 mmol). The resulting mixture was stirred at 90 °C for 18 h. After cooling, the solvents were removed under vacuum. The residue was diluted with CH₂Cl₂ (50 mL) and saturated aqueous NH₄Cl (70 mL). The aqueous layer was washed with CH₂Cl₂ (2 × 30 mL). The combined organic layers were washed with brine (50 mL) and dried with Na₂SO₄. After removal of the solvent under reduced pressure, the residue was purified by column chromatography (SiO₂, CHCl₃/ethyl acetate 1:1) to give the chromophore **3** as a yellow oil (252 mg, 0.620 mmol, 88%). ¹H NMR (500 MHz, CDCl₃): δ = 3.79 (s, 6H), 6.82–6.86 (m, 6H), 7.06–7.08 (m, 4H), 7.30–7.32 (m, 4H), 8.53–8.55 (m, 2H) ppm. ¹³C NMR (125 MHz, CDCl₃): δ = 55.7, 85.9, 95.5, 112.4, 115.1, 118.8, 125.5, 127.6, 132.2, 133.0, 139.9, 149.77, 149.82, 156.7 ppm. HRMS (MALDI) *m/z* calcd. for C₂₇H₂₂N₂O₂: 406.1676 [M⁺], found 406.1680. The spectroscopic data are consistent with those reported in the literature.³⁶

***N,N*-Bis[4-(9H-carbazol-9-yl)phenyl]-4-(pyridin-4-yl)aniline (4):** This compound was prepared according to the general procedure for Suzuki–Miyaura cross-coupling starting from compound **10** (200 mg, 0.306 mmol). Purification by column chromatography afforded the pure chromophore **4** as a yellow solid (112 mg, 0.171 mmol, 56%). ¹H NMR (500 MHz, CDCl₃): δ = 7.30–7.33 (m, 4H), 7.39–7.41 (m, 2H), 7.44–7.47 (m, 8H), 7.50–7.56 (m, 10H), 7.66–7.68 (m, 2H), 8.16–8.18 (m, 4H), 8.66–8.67 (m, 2H) ppm. ¹³C NMR (125 MHz, CDCl₃): δ = 110.0, 120.2, 120.6, 121.2, 123.5, 124.5, 125.7, 126.1, 128.4, 128.4, 132.74, 133.14, 141.1, 146.3, 147.6, 148.5, 150.5 ppm. HRMS (MALDI) *m/z* calcd. for C₄₇H₃₂N₄: 652.2621 [M⁺], found 652.2638.

(E)-N,N-Bis[4-(9H-carbazol-9-yl)phenyl]-4-[2-(pyridin-4-yl)vinyl]aniline (5): This compound was prepared according to the general procedure for Heck cross-coupling starting from compound **11** (200 mg, 0.29 mmol, 1 equiv.) and 4-vinylpyridine (39 mg, 0.37 mmol, 1.3 equiv). The crude product was purified by column chromatography (SiO₂; ethyl acetate). Yellow solid (80 mg, 41%); *R*_f = 0.6 (SiO₂; ethyl acetate). ¹H NMR (300 MHz, CDCl₃): δ = 6.98 (d, ³*J* = 16.5 Hz, 1H), 7.29–7.58 (m, 27H), 8.16–8.18 (m, 4H), 8.57–8.59 (m, 2H) ppm. ¹³C NMR (75 MHz, CDCl₃): δ = 109.9, 120.1, 120.5, 120.9, 123.5, 124.3, 125.0, 125.6, 126.1, 128.3, 128.5, 131.4, 132.5, 133.0, 141.1, 144.9, 146.3, 147.9, 150.3 ppm. HRMS (MALDI) *m/z* calcd. for C₄₉H₃₄N₄: 678.2778 [M⁺], found 678.2774.

4-(5-Methoxythiophen-2-yl)-N-[4-(5-methoxythiophen-2-yl)phenyl]-N-[4-(pyridin-4-yl)phenyl]aniline (6): This compound was prepared according to the general procedure for the Suzuki–Miyaura cross-coupling starting from compound **12** (200 mg, 0.365 mmol). Purification by column chromatography afforded the pure chromophore **6** as a yellow-orange solid (166 mg, 0.303 mmol, 83%). ¹H NMR (500 MHz, CDCl₃): δ = 3.90 (s, 6H), 6.16 (d, *J* = 4.0 Hz, 2H), 6.88 (d, *J* = 4.0 Hz, 2H), 7.09–7.10 (m, 4H), 7.16–7.17 (m, 2H), 7.37–7.39 (m, 4H), 7.46–7.47 (m, 2H), 7.51–7.53 (m, 2H), 8.60–8.61 (m, 2H) ppm. ¹³C NMR (125 MHz, CDCl₃): δ = 60.4, 104.9, 120.3, 121.1, 123.4, 125.2, 126.0, 127.9, 130.0, 130.3, 131.5, 145.7, 147.7, 148.6, 150.4, 165.8 ppm. HRMS (MALDI) *m/z* calcd. for C₃₃H₂₆N₂O₂S₂: 546.1430 [M⁺], found 546.1444.

Acknowledgements

This work was supported by the European Regional Development Fund-Project "High sensitive sensors and low density materials based on polymeric nanocomposites - NANOMAT (No. CZ.02.1.01/0.0/0.0/17_048/0007376)". J.R.-L. thanks the Ministerio de Economía y Competitividad/Agencia Estatal de Investigación/FEDER for financial support

(project CTQ2017-84561-P). Funding from the Junta de Comunidades de Castilla-La Mancha/FEDER is also gratefully acknowledged by J.R.-L. and S.A. (project SBPLY/17/180501/000214). M. F. thanks the Région Bretagne, France, for funding.

Keywords: Push-pull; Intramolecular charge transfer; Nitrogen heterocycles; Triphenylamine; Fluorescence

References

-
- ¹ (a) H. N. Kim, Z. Guo, W. Zhu, J. Yoon, H. Tian, *Chem. Soc. Rev.* **2011**, *40*, 79-93; (b) A. S. Klymchenko, *Acc. Chem. Res.* **2017**, *50*, 366-375.
- ² Y. Ohmori, *Laser Photonics Rev.* **2009**, *4*, 300-310.
- ³ (a) A. Mishra, P. Bäuerle, *Angew. Chem. Int. Ed.* **2012**, *51*, 2020-2067; (b) C. Duan, F. Huang, Y. Cao, *J. Mater. Chem. C* **2012**, *22*, 10416-10434; (c) B. Walker, C. Kim, T.-Q. Nguyen, *Chem. Mater.* **2011**, *23*, 471-782.
- ⁴ (a) M Liang, J. Chen, *Chem. Soc. Rev.* **2013**, *42*, 3453-4388; (b) Y. Wu, W. Zhu, *Chem. Soc. Rev.* **2013**, *4*, 2039-2058; (c) J. N. Clifford E. Martinez-Ferrero, A. Viterisi, E. Palomares, *Chem. Soc. Rev.* **2011**, *40*, 1635-1646.
- ⁵ (a) A. Facchetti, *Mater. Today* **2007**, *10*, 28-37; (b) H. Sirringhaus, *Adv. Mater.* **2014**, *26*, 1319-1335; (c) M. J. Malachowski, J. Zmija, *Opto-Electron. Rev.* **2010**, *18*, 121-136.
- ⁶ (a) M. Pawlicki, H. A. Collins, R. G. Denning, H. L. Anderson, *Angew. Chem. Int. Ed.* **2009**, *48*, 3244-3266; (b) G. S. He, L.-S. Tan, Q. Zheng, P. N. Prasad *Chem. Rev.* **2008**, *108*, 1245-1330; (c) J. Liu, W. Gao, I. Kityk, X. Liu, Z. Zhen, *Dyes Pigm.* **2015**, *122*, 74-84.
- ⁷ F. Bureš, *RSC Adv.* **2014**, *4*, 58826-58851.
- ⁸ (a) C. Moreno-Yruela, J. Garín, S. Orduna, E. Quintero, J. T. López Navarrete, B. E. Diosdado, B. Villacampa, J. Casado, and R. Andreu, *J. Org. Chem.* **2015**, *80*, 12115-12128;

(b) P. Solanke, S. Achelle, N. Cabon, O. Pytela, A. Barsella, B. Caro, F. Robin-le Guen, J. Podlesny, M. Klikar and F. Bureš, *Dyes Pigm.*, **2016**, 134, 129-138.

⁹ (a) R. Wu, L. Yin, Y. Li, *Sci. China Mater.* **2016**, 59, 371-388; (b) K. Hoffert, R. J. Durand, S. Gauthier, F. Robin-le Guen, S. Achelle, *Eur. J. Org. Chem.* **2017**, 523-529; (c) M. Klikar, F. Bureš, O. Pytela, T. Mikysek, Z. Padělková, A. Barsella, K. Dorkenoo, S. Achelle, *New J. Chem.* **2013**, 37, 4230-4240.

¹⁰ (a) M. Klikar, P. Solanke, J. Tydlitát, F. Bureš, *Chem. Rec.* **2016**, 16, 1886-1905; (b) C. Katan, S. Tretiak, M. H. V. Werts, A. J. Bain, R. J. Marsh, N. Leonczek, N. Nicolaou, E. Badaeva, O. Mongin, M. Blanchard-Desce *J. Phys. Chem. B* **2007**, 111, 9468-9483.

¹¹ (a) N. Sun, S. Meng, D. Chao, Z. Zhou, Y. Du, D. Wang, X. Zhao, H. Zhou, C. Chen, *Polym. Chem.* **2016**, 7, 6055-6063; (b) C. Wu, Z. Wu, B. Wang, X. Li, N. Zhao, J. Hu, D. Ma, Q. Wang, *ACS Appl. Mater. Interfaces* **2017**, 9, 32946-32956; (c) X. J. Feng, J. Peng, Z. Xu, R. Fang, H. Zhang, X. Xu, L. Li, J. Gao, M. S. Wong, *ACS Appl. Mater. Interfaces* **2015**, 7, 2856-28165; (d) S. Achelle, A. Barsella, B. Caro, F. Robin-le Guen, *RSC Adv.* **2015**, 5, 39218-39227.

¹² (a) S. Achelle, S. Kahlal, A. Barsella, J.-Y. Saillard, X. Che, J. Vallet, F. Bureš, B. Caro, F. Robin-le Guen, *Dyes Pigm.* **2015**, 113, 562-570; (b) M. Klikar, P. le Poul, A. Růžička, O. Pytela, A. Barsella, K. D. Dorkenoo, F. Robin-le Guen, F. Bureš, S. Achelle, *J. Org. Chem.* **2017**, 82, 9435-9451; (c) Z. Pokladek, N. Ripoche, M. Betou, Y. Trolez, O. Mongin, J. Olesiak-Banska, K. Matczyszyn, M. Samoc, M. G. Humphrey, M. Blanchard-Desce, F. Paul, *Chem. Eur. J.* **2016**, 22, 10155-10167.

¹³ (a) W.-J. Shi, T. Kinoshita, D. K. P. Ng, *Asian J. Org. Chem.* **2017**, 6, 1476-1485; (b) P. Ferdowsi, Y. Saygili, W. Zhang, T. Edvinson, L. Kavan, J. Mokhtari, S. M. Zakeeruddin, M. Gratzel, A. Hagfeldt, *ChemSusChem* **2018**, 11, 494-502; (c) L.-Y. Lin, C.-H. Twai, K.-T.

Wong, T.-W. Huang, C.-C. Wu, S.-H. Chou, F. Lin, S.-H. Chen, A.-I Tsai, *J. Mater. Chem.* **2011**, *21*, 5950-5958.

¹⁴ O. Kwon, S. Barlow, S. A. Odom, L. Beverina, N. J. Thompson, E. Zojer, J.-L. Brédas, S. R. Marder, *J. Phys. Chem. A* **2005**, *109*, 9346-9352.

¹⁵ (a) I. Malina, V. Kampars, B. Turovska, S. Belyakov, *Dyes Pigm.* **2017**, *139*, 820-830; (b) H. Agnihotri, P. Mahalingevelar, H. Mande, P. Ghalsasi, S. Kanvah, *Dyes Pigm.* **2015**, *123*, 341-348.

¹⁶ (a) C. Katan, S. Tretiak, M. H. V. Werts, A. J. Bain, R. J. Marsh, N. Leonczek, N. Nicolaou, E. Badaeva, O. Mongin, M. Blanchard-Desce, *J. Phys. Chem. B* **2007**, *111*, 9468-9483; (b) D. Cvejn, E. Michail, K. Seintis, M. Klikar, O. Pytela, T. Mikysek, N. Amonasy, M. Ludwig, V. Giannetas, M. Fakis, F. Bureš, *RSC Adv.* **2016**, *6*, 12819-12828; (c) M. Klikar, K. Seintis, I. Polyzos, O. Pytela, T. Mikysek, N. Almonasy, M. Fakis, F. Bureš, *ChemPhotoChem* **2018**, *2*, 465-474.

¹⁷ (a) J. Weng, Q. Mei, Q. Fan, Q. Ling, B. Tong, W. Huang, *RSC Adv.* **2013**, *3*, 21877-21887; (b) S. Easwaramoorthi, P. Thamaraiselvi, K. Duraimurugan, A. J. Beneto, A. Siva B. U. Nair, *Chem. Commun.*, **2014**, *50*, 6902-6905.

¹⁸ (a) Z. He, C.-W. Kan, C.-L. Ho, W.-Y. Wong, C.-H. Chui, K.-L. Tong, S.-K. So, T.-H. Lee, L. M. Leung, Z. Lin, *Dyes Pigm.* **2011**, *88*, 333-343; (b) Z. Zhang, Y. Zheng, Z. Sun, Z. Dai, Z. Tang, J. Ma, C. Ma, *Adv. Synth. Catal.* **2017**, *359*, 2259-2268; (c) D. Gudeika, A. Bundulis, I. Mihailovs, D. Volyniuk, M. Rutkis, J. V. Grazulevicius, *Dyes Pigm.* **2017**, *140*, 431-440.

¹⁹ (a) M. W. Thesen, B. Höfer, M. Debeaux, S. Janietz, A. Wedel, A. Köhler, H.-H. Johannes, H. Krueger, *J. Polym. Sci. A Polym. Chem.* **2010**, *48*, 3417-3430; (b) P. B. Pati, S. S. Zade, *Tetrahedron Lett.* **2014**, *55*, 5290-5293.

-
- ²⁰ (a) G.-G. Shan, H.-B.; Li, J.-S. Qin, D.-X. Zhu, Y. Liao, Z.-M. Su, *Dalton Trans.* **2012**, *41*, 9590-593; (b) B. Pan, H. Huang, X. Yang, J. Jin, S. Zhuang, G. Mu, L. Wang, *J. Mater. Chem. C* **2014**, *2*, 7428-7435; (c) Y. Jin, Y. Qian, *New J. Chem.* **2015**, *39*, 2872-2880.
- ²¹ (a) D. S. Kopchuk, A. P. Krinochin, E. S. Starnovskaya, Y. K. Shtaitz, A. F. Khasanov, O. S. Taniya, S. Santra, G. V. Zyryanov, A. Majee, V. L. Rusinov, O. N. Chupakhin, *Chem. Select* **2018**, *3*, 4141-4146; (b) C. Coluccini, M. Cariato, E. Cariati, S. Righetto, A. Forni, D. Pasini, *RSC Adv.* **2015**, *5*, 21495-21503; (c) Y. Qian, M. Luo, *Dyes Pigm.* **2014**, *101*, 240-246; (d) E. Cariati, C. Dragonetti, E. Lucenti, F. Nisic, S. Righetto, D. Roberto, E. Tordin, *Chem. Commun.* **2014**, *50*, 1608-1610; (e) R. Li, Z.-L. Gong, J.-H. Tang, M.-J. Sun, J.-Y. Shao, Y.-W. Zhong, J. Yao, *Sci. China Chem.* **2018**, *61*, 545-556.
- ²² (a) J. Ma, W. Li, J. Li, R. Shi, G. Yin, R. Wang, *Talanta*, **2018**, *182*, 464-469; (b) V. Kachwal, P. Alarn, H. R. Yadav, S. S. Pasha, A. R. Choudhury, I. R. Laskar, *New J. Chem.* **2018**, *42*, 1133-1140.
- ²³ J. Tydlitát, S. Achelle, J. Rodríguez-López, O. Pytela, T. Mikýsek, N. Cabon, F. Robin-le Guen, D. Miklik, Z. Růžicková, F. Bureš, *Dyes Pigm.* **2017**, *145*, 467-478.
- ²⁴ C. Allain, F. Schmidt, R. Lartia, G. Bordeau, C. Fiorini-Debuisschert, F. Charra, P. Tauc, M.-P. Teulade-Fichou, *ChemBioChem* **2007**, *8*, 424-433.
- ²⁵ S.-i. Kato, Y. Yamada, H. Hiyoshi, K. Umezu, Y. Nakamura, *J. Org. Chem.* **2015**, *80*, 9076-9090.
- ²⁶ D. F. Eaton, *Pure Appl. Chem.* **1988**, *60*, 1107-1114.
- ²⁷ (a) R. Lartia, C. Allain, G. Bordeau, F. Schmidt, C. Fiorini-Debuisschert, F. Charra, M.-P. Teulade-Fichou, *J. Org. Chem.* **2008**, *73*, 1732-1744; (b) F. Mahuteau-Betzer, S. Piguel, *Tetrahedron Lett.* **2013**, *54*, 3188-3193; (c) S. Achelle, F. Robin-le Guen, *J. Photochem. Photobiol. A* **2017**, *348*, 281-286.
- ²⁸ C. Reichardt, *Chem. Rev.* **1994**, *94*, 2319-2358.

²⁹ D. Bao, B. Millare, W. Xia, B.G. Steyer, A.A. Gerasimenko, A. Ferreira, A. Contreras, V. I. Vullev *J. Phys. Chem. A* **2009**, *113*, 1259-1267.

³⁰ M. J. Frisch, G. W. Trucks, H. B. Schlegel, G. E. Scuseria, M. A. Robb, J. R. Cheeseman, G. Scalmani, V. Barone, G. A. Petersson, H. Nakatsuji, X. Li, M. Caricato, A. V. Marenich, J. Bloino, B. G. Janesko, R. Gomperts, B. Mennucci, H. P. Hratchian, J. V. Ortiz, A. F. Izmaylov, J. L. Sonnenberg, D. Williams-Young, F. Ding, F. Lipparini, F. Egidi, J. Goings, B. Peng, A. Petrone, T. Henderson, D. Ranasinghe, V. G. Zakrzewski, J. Gao, N. Rega, G. Zheng, W. Liang, M. Hada, M. Ehara, K. Toyota, R. Fukuda, J. Hasegawa, M. Ishida, T. Nakajima, Y. Honda, O. Kitao, H. Nakai, T. Vreven, K. Throssell, J. A. Montgomery, Jr., J. E. Peralta, F. Ogliaro, M. J. Bearpark, J. J. Heyd, E. N. Brothers, K. N. Kudin, V. N. Staroverov, T. A. Keith, R. Kobayashi, J. Normand, K. Raghavachari, A. P. Rendell, J. C. Burant, S. S. Iyengar, J. Tomasi, M. Cossi, J. M. Millam, M. Klene, C. Adamo, R. Cammi, J. W. Ochterski, R. L. Martin, K. Morokuma, O. Farkas, J. B. Foresman, and D. J. Fox, Gaussian, Inc., Wallingford CT, 2016.

³¹ A. C. Spivey, L. Shukla, J. D. Hayler *Org. Lett.* **2007**, *9*, 891-894.

³² OPchem, O. Pytela, version 8.3, webpage: <http://bures.upce.cz/OPgm/>

³³ C. Lambert, G. Nöll, E. Schmäzlin, K. Meerholz, C. Bräuchle, *Chem. Eur. J.* **1998**, *4*, 2129-2135.

³⁴ S. Mathew, H. Imahori, *J. Mater. Chem.* **2011**, *21*, 7166-7174.

³⁵ Y. Hua, B. Xu, P. Liu, H. Chen, H. Tian, M. Cheng, L. Kloob, L. Sun, *Chem. Sci.* **2016**, *7*, 2633-2638.

³⁶ C. Lambert, W. Gaschler, G. Nöll, M. Weber, E. Schmäzlin, C. Bräuchle, K. Meerholz, *J. Chem. Soc., Perkin Trans. 2* **2001**, 964-974.